A Rapidly Deployable Wave Energy Converter for Seawater Desalination in Disaster Response

Ryan W. Weed, and Bridgette K. Hyde

Abstract—In the current operational landscape, there are no commercial-off-the-shelf (COTS) solutions capable of using wave power to produce clean water on a small scale and expedited timeline. Available wave-powered installations and desalination plants are mostly large infrastructure projects that leverage economies of scale. This is typically the result of economic drivers - the availability and price of electrical power and clean water. However, natural disasters often strike where clean water is scarce and local infrastructure is unable to respond quickly, driving an urgent need for clean water in locations far from large installations. Here, we present the design, modelling, and initial performance of a compact Wave-Energy-Converter (WEC) powering a reverse osmosis desalination system; a simple technical solution that provides clean water on a small scale (~1,000 Liters per day) and is quickly deployable in disaster response.

 ${\it Keywords-} wave \ {\it energy} \ converter, \ {\it desalination, disaster} \\ {\it response}$

I. INTRODUCTION

he impact of climate change to coastal communities is expected to increase in the coming decades [1]. Destructive storms and acute coastal events are likely to degrade local power grids and freshwater distribution. Correspondingly, an effective response to coastal disasters requires external sources of electricity and water that can be rapidly deployed to meet the need [2].

Wave Energy Converters (WEC) have received more recent attention as a possible source of renewable energy and to support disaster response near coastal areas [3]. The Department of Energy (DOE) and the National Renewable Energy Laboratory (NREL) recognized the lack of available wave powered desalination systems in the size range applicable to small community disaster response.

Part of a special issue for AWTEC 2024. Manuscript submitted 17 November 2024; Revised 20 September 2025; Accepted 13 October 2025. Published 20 October 2025.

This is an open access article distributed under the terms of the Creative Commons Attribution 4.0 International license. CC BY https://creativecommons.org/licenses/by/4.0/. Unrestricted use (including commercial), distribution and reproduction is permitted provided that credit is given to the original author(s) of the work, including a URI or hyperlink to the work, this public license and a copy right notice. This article has been subject to a single-blind peer review by a minimum of two reviewers.

R. Weed and B. Hyde are founders of Field Office Creative, San Francisco, CA 94107 email (ryanweed@gmail.com)

Digital Object Identifier: https://doi.org/10.36688/imej.8.417-424

In 2019, the Wave Power Technology Office (WPTO) sponsored the 'Waves to Water' Competition in order to spur commercial development of small wave powered desalination systems [4].

The 'Waves to Water' prize incentivized the development of small, modular, wave-powered desalination systems. This project required applicants to leverage numerical modelling tools; study advanced materials that can be easily packaged, transported, and assembled; and develop metrics that could quantify the performance of both electricity producing and non-electricity producing wave powered desalination systems.

The WEC and desalination system presented here was designed in response to the 'Wates to Water' prize competition and advanced to the final stage of in-water competition held at Jennette's Pier in Nags Head, North Carolina, in partnership with the Coastal Studies Institute and Eastern Carolina University.

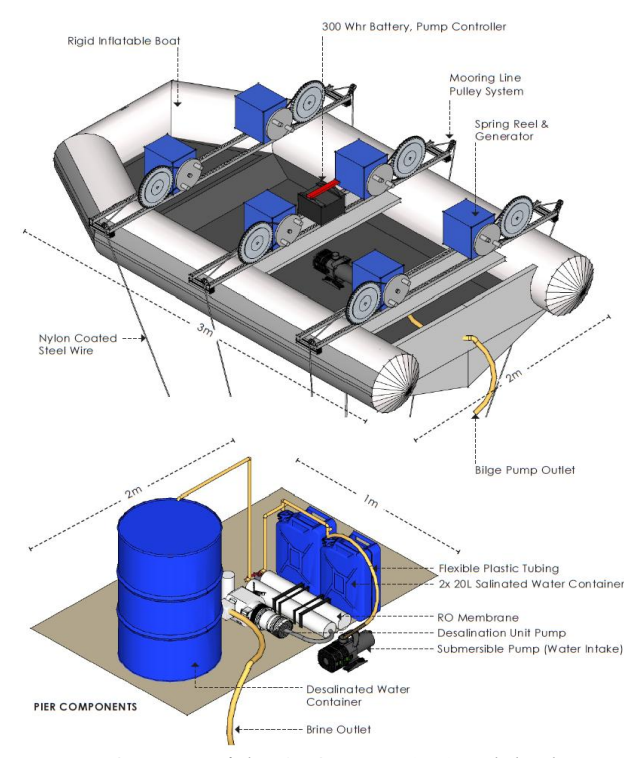


Fig. 1. Overview of the WEC system (top) and desalination system (bottom).

II. SYSTEM OVERVIEW

The WEC system design illustrated in Figures 1 and 2 houses several commercial-off-the-shelf (COTS) 3-phase

generators mounted on an inflatable boat. The generators are attached to a retractable reel via chain and gearing, which is in turn anchored to the sea floor. As ocean waves move the boat, the spring reel cable pulley is constantly wound and unwound. This action turns the generator and provides periodic electricity to the battery.

To account for tidal variations, the power take-off (PTO) mechanisms are mounted onto linear guide rails with adjustable ballscrew mechanisms.

As the tidal height increases or decreases, a motor turns the ballscrew and the PTOs move along the guide rails, adjusting the effective length of the tension lines. The PTO position is determined based on real-time GPS position measurements and predicted tidal variations for a given location.

A flywheel is attached to the generator shaft, along with a freewheel gear mechanism, ensuring that the generator is engaged only as the cable pulley is extended. The inertia of the flywheel also helps stabilize the energy produced by the generator. Even with the flywheel, the limited battery charging power capability will require the use of a supercapacitor to absorb the short period (seconds) higher power peak pulses of generator output in the more energetic wave sea states. The 64F/64V capacitor can store up to 100kJ, capable of absorbing the peak generator output (up to 4 kW) and discharging into the battery over a longer period at high DC-DC efficiency. The DC load controller monitors battery charge state and initiates the desalination unit when the battery is fully charged. Likewise, when the DC load controller senses the battery is approaching low voltage state, it shuts off the desalination unit to allow for recharging of the battery. A DC-DC buck converter on each generator converts low

current draw required from the WEC boat to the desalination system. The reduced current helps lower the cable losses and reduces cable mass.

Modular in nature, the complete WEC and desalination system is disassembled into a single 1.2m x 1m x 0.9m container that can be transported using a standard truckbed with a total system mass (M_{raft}) of approximately 500kg.

III. MODELLING APPROACH

At its simplest, the WEC is a forced spring-damper system. The forcing function is provided by the incoming wave motion and the buoyancy effect of the inflatable boat. Mechanical energy is captured by a geared spring reel/generator system (PTO). The PTO's produce power as the mooring lines are extended and retracted, based on movement of the boat in vertical (heave), horizontal (surge) and pitch.

A. Physics Model

Our objective was to use simple physics-based models of forces (spring, buoyancy, drag) and include realistic constants/coefficients to increase the model fidelity as much as possible, comparing the model output with full-scale system testing data to validate the model. We included the mechanics of the WEC using a 3 degree-of-freedom (3DOF) forced/damped oscillator. This included modelling of dynamics of the WEC boat in heave, surge (lateral) and pitch.

TABLE 1. EXPECTED WAVE CHARACTERISTICS AND DURATIONS FOR MODELLING.

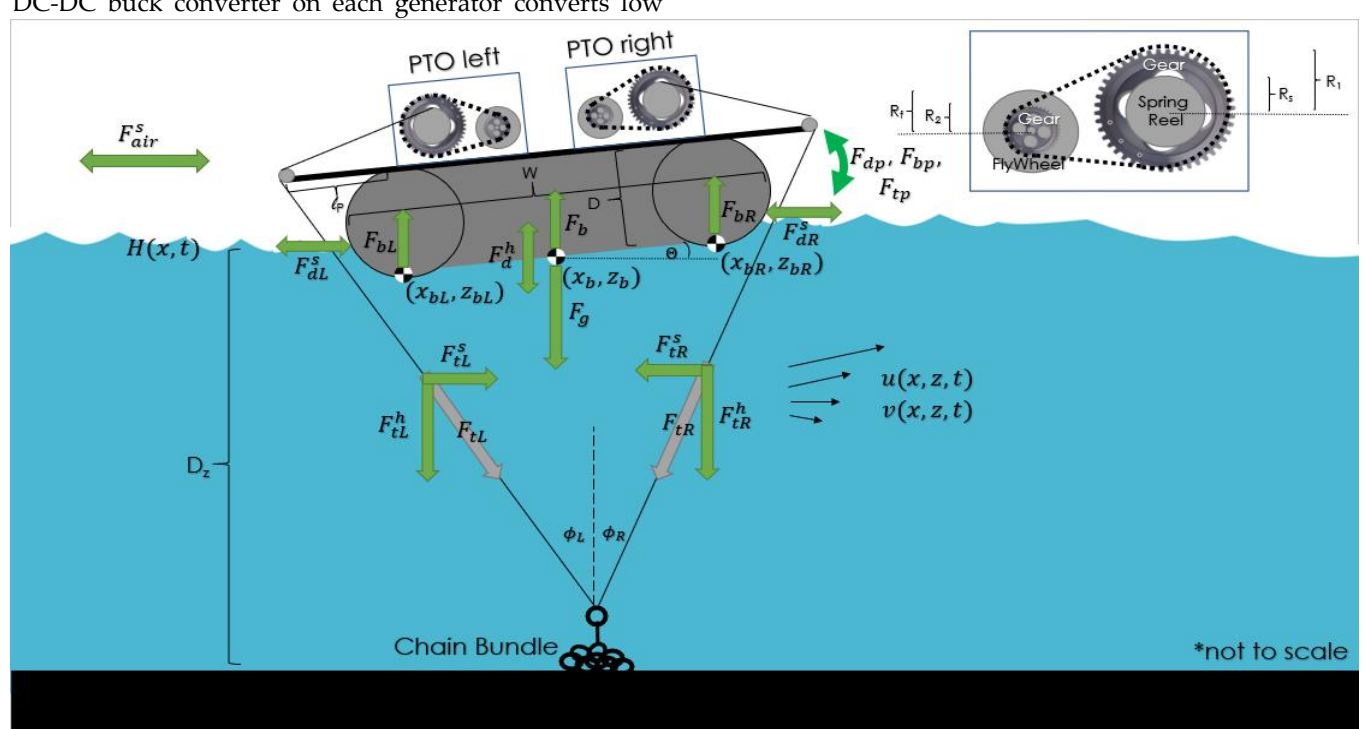


Fig. 2. Overview of the 3DOF modelling setup. PTO component dimensions are shown in the top right inset. Green arrows indicate the various forces on the WEC.

Sea State	Significant Wave Height	Energy Period	Duration
W1	0.5 m	6 sec	(22%)
W2	0.5 m	10 sec	(5%)
W3	1.0 m	6 sec	(28%)
W4	1.5 m	7 sec	(22%)
W5	2.0 m	7 sec	(22%)
W6	3.0	7 sec	(1%)

In this model (Fig. 2), the heave, surge, and pitch forces acting on the WEC boat are:

$$F_{heave} = M_h \ddot{z} = F_G + F_b + F_d^h + F_t^h$$
 (1)

$$F_{surge} = M_s \ddot{x} = F_d^s + F_{air}^s + F_t^s$$
 (2)

$$F_{pitch} = I_r \ddot{\theta} = F_d^p + F_t^p + F_b^p$$
 (3)

$$F_{surge} = M_s \ddot{x} = F_d^s + F_{air}^s + F_t^s \tag{2}$$

$$F_{nitch} = I_r \ddot{\theta} = F_d^p + F_t^p + F_h^p \tag{3}$$

Where M_h and M_s are the WEC boat mass, including added hydrodynamic acceleration mass (see section D for description) in heave and surge, respectively. $F_G =$ $-M_{raft}g$ is the gravitational force, and F_b is the buoyant force from the waves. The hydrodynamic drag is expressed in F_d^s , F_d^p and F_d^h for surge, pitch, and heave, respectively. F_t^s , F_t^p , and F_t^h describe the line tension force in surge, pitch, and heave, respectively. Aerodynamic drag force is F_{air}^s . The average water depth is D_z , and the wave surface height is H(x,t) with water horizontal and vertical velocities given by u(x, z, t) and v(x, z, t), respectively. I_r is the moment of inertia of the WEC boat, approximated by:

$$I_r = \frac{12}{M_p(L^2 + D^2)} \tag{4}$$

Where M_n is the acceleration mass in the pitch axis (see section D for description).

The WEC boat body position is described by (x_h, z_h, θ) , with the left- and right-side positions described by: $x_{bL} =$ $x_b - \frac{w}{2}\cos(\theta)$ and $x_{bR} = x_b + \frac{w}{2}\cos(\theta)$. The angle between vertical axis and the tension lines is given by $\phi_L =$ atan $\left[\frac{x_{bL}}{z_{bL}}\right]$ and $\phi_R = \operatorname{atan}\left[\frac{x_{bR}}{z_{bR}}\right]$.

C. Wave Characteristics

We use shallow water linear wave approximation [5] to determine wave heights, frequency, and velocities for the ith mode:

$$H_i(x,t) = A_i \cos(k_i x - \omega_i)$$
 (5)

$$\omega_i = \sqrt{gD_z k_i} \tag{6}$$

$$u_i(x, z, t) = \frac{A_i \omega_i}{R_i k} \cos(k_i x - \omega_i t) \tag{7}$$

$$\omega_{i} = \sqrt{gD_{z}}k_{i}$$
 (6)

$$u_{i}(x,z,t) = \frac{A_{i}\omega_{i}}{D_{z}k_{i}} \cos(k_{i}x - \omega_{i}t)$$
 (7)

$$v_{i}(x,z,t) = \frac{A_{i}\omega_{i}z}{D_{z}} \sin(k_{i}x - \omega_{i}t)$$
 (8)

Where A_i , ω_i , k_i is the amplitude, frequency, and wave number for the ith mode.

The modeling output is estimated using a timedomain model assuming a Bretschneider wave spectrum [10] as defined below:

$$S(\omega) = \frac{5}{16} \frac{\omega_m^4}{\omega^5} H_S^2 e^{-5\omega_m^4/4\omega^4}$$
 (9)

Where ω is the wave frequency, in radians per second, and ω_m is the most likely frequency of any given wave and H_s is the significant wave height in meters.

Fourier integrals allow us to transfer between the Bretschneider frequency domain and wave heights in the time domain. The wave spectrum is broken into 6 specific sea-states based on expected wave characteristics for WEC deployment sites (see Table 1).

These sea states (W1-W6) are shown in Fig. 3 in frequency domain and Fig. 4 in time-domain. In general, we see heave velocities below +/- 2m/s, well within the operational range of the PTO's with a gear ratio of 10.

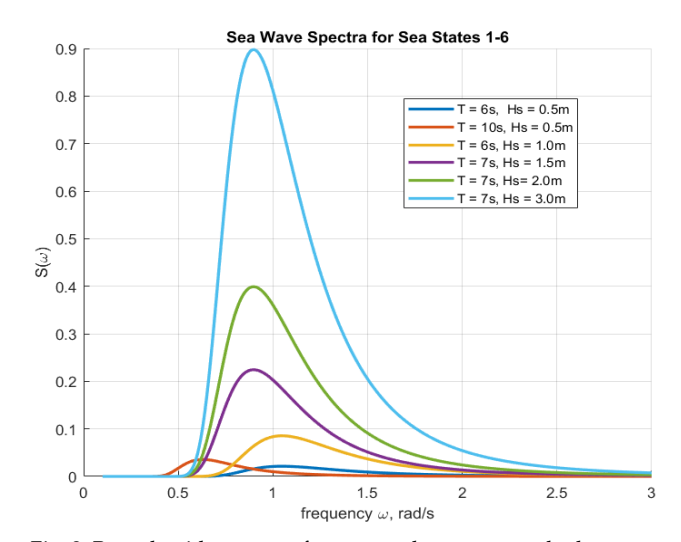


Fig. 3. Bretschneider spectra for expected sea states at deployment location.

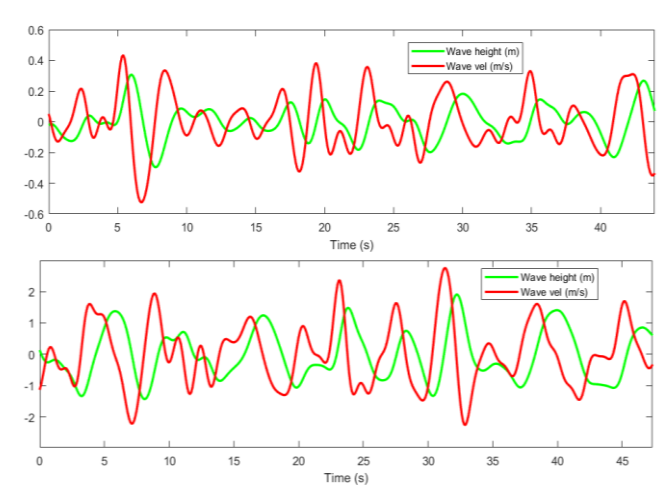


Fig. 4. Bretschneider time series wave amplitude and velocities for W1 (top) and W6 (bottom) expected Sea states at deployment location.

D. Forces on the WEC

Line Tension: The spring force on the left and right side F_{kL} and F_{kR} is proportional to the extension of the spring reels, $dS_{L/R}$:

$$F_{kL/R} = N_s k_s (dS_{L/R}) = N_s k_s (\sqrt{x_{bL/R}^2 + z_{bL/R}^2} - \delta)$$
 (10)

Where N_s is the number of spring reels on each side of the WEC boat and δ is the static length of line from mooring attachment to the end of spring reel cable. The spring constant k_s comes from the manufacturer specification of the spring reel ($k_s = 80N/m$). Linear drag due to the PTO generator is expressed in:

$$F_{PTO} = -b * \frac{d}{dt} \left[dS_{\frac{L}{R}} \right] - F_{gen} \tag{11}$$

where the linear drag coefficient b was measured to be 12.6Ns/m for a single PTO. The F_{gen} value describes the input torque to the generator under load. While this specification at low rpm's was not available from the manufacturer, we model the input torque using a function:

$$F_{aen} = c[ln(rpm) - 1] \tag{12}$$

Where *rpm* is generator revolutions per minute, related to cable extension and retraction by:

$$rpm_{L/R} = \frac{60R_1 \frac{d}{dt} \left[dS_L \right]}{2\pi R_S R_2} \tag{13}$$

Using W/rpm specification from the generator in our PTO and combining the input torque specification from similar 3-phase permanent magnet alternators, we estimate the input torque constant $c \sim 0.05$ for modeling purposes.

The total line tension on the left and right-side PTO cables is given by:

$$F_{tL/R} = F_{kL/R} + F_{fL/R} + (F_{PTO})_{L/R}$$
 (14)

Where $F_{fL/R} = I_f \frac{R_1}{(R_2 R_S)^2} \frac{d^2}{dt^2} \left[dS_{L/R} \right]$ is the force on the cables due to the rotational inertia of the flywheel with inertial mass, $I_f = N_S \frac{M_f}{2} \left[R_i^{\ 2} + R_e^{\ 2} \right]$.

Here, M_f is the total flywheel mass and R_i and R_e are the inner and outer radii, respectively.

The heave and surge components of the tension forces are $(F_t^h)_{L/R} = F_{tL/R}cos(\phi_{L/R})$ and $(F_t^s)_{L/R} = F_{tL/R}sin(\phi_{L/R})$, respectively. The pitch force due to the tension lines is given by:

$$F_t^p = \frac{w}{2} [F_{tL} cos(\phi_L + \theta) - F_{tR} cos(\phi_R + \theta)]. \tag{15}$$

Drag: We consider both aerodynamic drag, F_{air}^s and hydrodynamic drag forces (F_d^s, F_d^h, F_d^p) on the WEC boat. Drag forces due to wind on the floating structure are

assumed to act in surge direction only and are approximated by:

$$F_{air}^s = \frac{1}{2} \rho_a \ell D C_a |V_a| V_a \tag{16}$$

Where ρ_a is the density of air (approximately 816 times less dense than water), C_a is the drag coefficient, V_a is the wind speed, ℓ and D is the boat length and depth, respectively.

Drag forces due to relative motion between WEC boat and surrounding water causes hydrodynamics drag in heave, surge, and pitch directions. We have assumed that the hydrodynamic drag for the WEC buoy/boat follows the form of:

$$F_D = \frac{1}{2} \rho A C_w v^2 \tag{17}$$

where ρ is the density of water at 25°C (1020 $\frac{\text{kg}}{\text{m}^3}$), A is the cross-section area of the buoy/boat, and v is the relative velocity of the water. We assume $C_w = 0.5$. This is consistent with similar shapes and relative water velocities that have been measured experimentally [6].

In the surge direction, the total drag force, $F_d^s = (F_d^s)_L + (F_d^s)_R$, where:

$$(F_d^s)_{L/R} = \frac{1}{2} \rho_w C_w [H(x_{bL/R}) - z_{bL/R}] \ell \left| u(x_{bL/R}, z_{bL/R}) - \frac{d}{dt} (x_{bL/R}) \right| \left(u(x_{bL/R}, z_{bL/R}) - \frac{d}{dt} (x_{bL/R}) \right)$$
(18)

Where ρ_w is the density of salt-water and C_w is the drag coefficient of the WEC boat shape. Similarly, the hydrodynamics drag in the heave direction is given by:

$$(F_d^h)_{L/R} = \frac{1}{2} \rho_W C_W W \ell \left| v(x_{bL/R}, z_{bL/R}) - \frac{d}{dt} (z_{bL/R}) \right| \left(v(x_{bL/R}, z_{bL/R}) - \frac{d}{dt} (z_{bL/R}) \right)$$
 (19)

In the pitch axis, the hydrodynamic drag is approximated:

$$F_d^p = -\frac{W^3}{8} \rho_w W C_w \left| \frac{d}{dt}(\theta) \right| \frac{d}{dt}(\theta)$$
 (20)

For aerodynamic drag coefficient, we have assumed $C_a = 0.5$, which is consistent with the somewhat ellipsoid like shape of the WEC boat 'leading-edges' [7].

Because of the unsteady motion of the WEC boat on the waves, we must consider the acceleration of the surrounding fluid in simulating the dynamics of motion. This is typically incorporated as an 'added mass' in the equations of motion. For modeling, we will approximate the shape of the WEC boat as a spheroid with length W and depth D and use the added mass calculation of Newman [8] to estimate this effect.

Using the geometry of the WEC boat, the length-to-width factor is approximately 0.3, which leads to added mass factors of 0.1, 0.8, and 0.5 for heave, surge, and pitch,

respectively [8]. For the equations of motion, the WEC boat mass is:

$$M_h = 1.1 M_{raft}$$

$$M_s = 1.8 M_{raft}$$

$$M_p = 1.5 M_{raft}$$

$$v(x, z, t) = \sum_{i=1}^{N} v_i(x, z, t)$$
 (27)

Where the ith mode wave amplitudes were given by the Bretschneider spectrum, $A_i = \sqrt{\frac{S(\omega_i)}{2}}$.

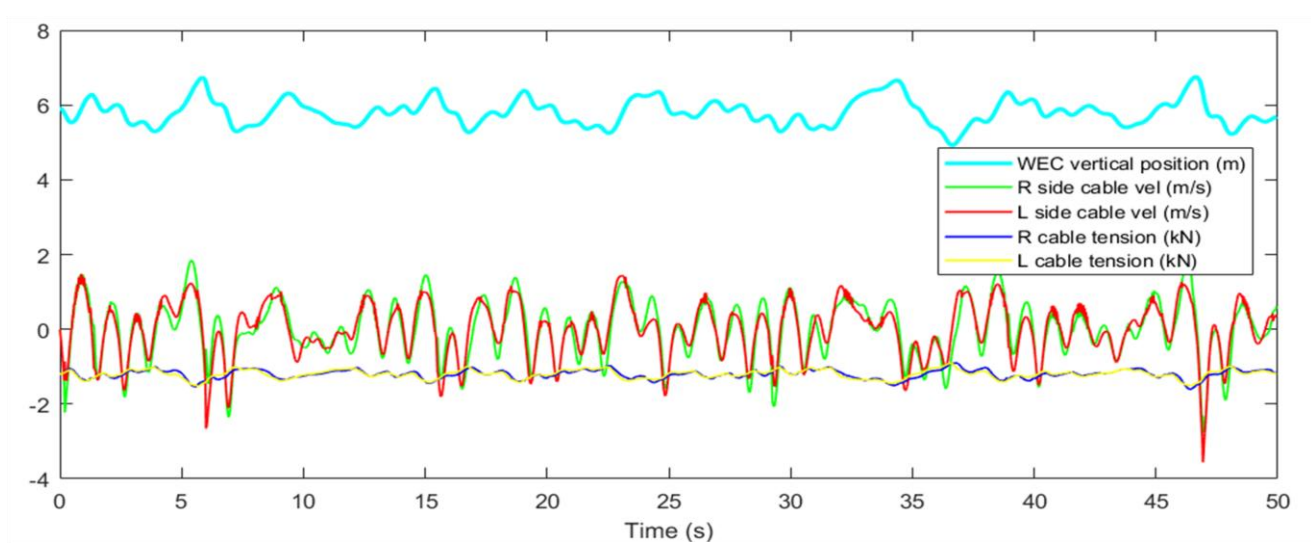


Fig. 5. Showing simulated dynamics of the WEC boat in the W4 wave state over 50 seconds of simulation.

Buoyancy: In this model we include buoyancy forces in the heave direction, as well as the possibility of pitching moments generated asymmetric buoyancy forces between left and right side of the WEC boat. As such, the heave and pitch forces due to buoyancy are given by:

$$F_b^h = \rho_w \ell g [A_L + A_R]$$

$$F_b^p = \frac{W \rho_w \ell g}{2} [A_R - A_L]$$
(21)

Where the 'wetted area' on the left and right side of the WEC boat is approximated by:

$$A_{L} = \frac{w}{4} [(H(x_{bL}) - z_{bL}) + (H(x_{b}) - z_{b})]$$

$$A_{R} = \frac{w}{4} [(H(x_{bR}) - z_{bR}) + (H(x_{b}) - z_{b})]$$
(23)

E. 3DOF Model Results

A MATLAB differential equation solver (ODE15s) is used to solve the system of differential equations (Equations 1-3) in the time domain. The physics-based model output was used to estimate how the WEC system responds to a given wave characteristic. The wave characteristics in the simulation domain were determined by a discrete sampling of the Bretschneider spectrum (Equation 9) combined with the shallow water linear wave assumptions in Equations 5-8, such that the wave height and velocity field were calculated by:

$$H(x,t) = \sum_{i=1}^{N} H_i(x,t) = \sum_{i=1}^{N} A_i \cos(k_i x - \omega_i t)$$
 (25)

$$u(x, z, t) = \sum_{i=1}^{N} u_i(x, z, t)$$
 (26)

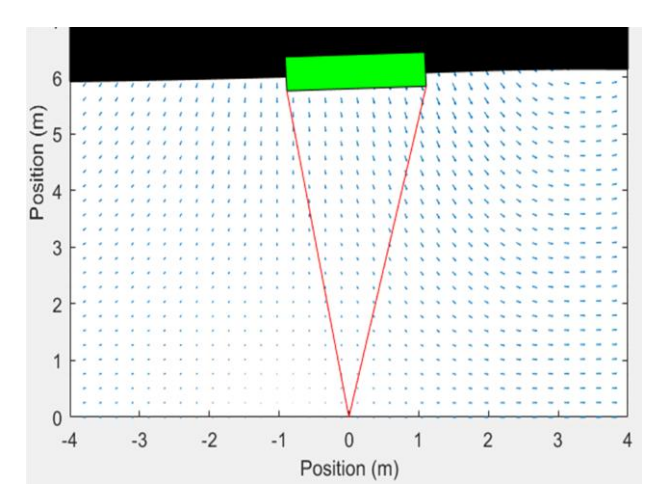


Fig. 6. Showing a freeze frame of the MATLAB animation output of the WEC boat dynamics in W4 sea state, as well as the surrounding water velocity field.

The resulting shallow-water vector field (Fig. 6) behaved as expected – the wave velocities followed an elliptical pattern in time, with the vertical velocity component v(x,z,t) dropping to zero near the seabed. Additionally, the significant wave height values were close to 4*s(H(x,t)), where s is the standard deviation from mean depth.

Using discrete sampling of the Bretschneider spectrum to build the wave states required simulations to be run in serial to reach 2000s simulation times and avoid undersampling of the frequency domain.

Fig. 5 shows a typical modeling simulation output. The total line tensions are consistently in the kN range per side (<kN per cable), and do not show large and/or rapid variations, which reflects positively for system safety and reliability. The asymmetry in the cable

extension/retraction velocity is due to the freewheel mechanism of the PTO, which only engages the generator during extension, leading to fast retraction velocities. This is modeled in the ODE solver with a non-stiff Heaviside function approximation.

Sea state W6 is the most vulnerable to heave velocities that can cause the vessel to swamp in extreme cases. We used the physics model to estimate this effect, looking at the change in draft position or waterline (ΔS) relative to the WEC boat at various frequency and weight combinations. The limiting case of sea state W6 can produce a 3.5m amplitude wave at an effective period of 4 seconds. Despite this, the maximum ΔS is approximately 0.2m. Since the average draft is 0.2m and the keel to top of hull position on the inflatable rigid boat is 0.7m, this gives us confidence that the boat will not onboard water during the most extreme wave conditions.

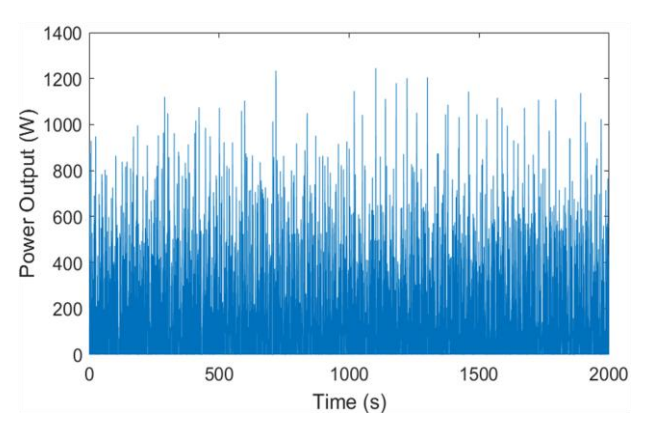


Fig. 7. A 2000s 3DOF model output of the WEC Power during sea state W4.

F. WEC Power Output

TABLE 2. 3DOF WEC MODELLING RESULTS FOR 6 EXPECTED SEA STATES.

TABLE 2. OBOT WEE MODELLING RESCRIPTION OF EAR ECTED SENTITIES.				
Sea State	Avg Absorbed Power [W]	Peak Absorbed Power [W]	Peak Mooring Loads [N]	
W1	102.2	486	2630	
W2	40.1	338	2590	
W3	212.9	906	2910	
W4	261.5	1511	3070	
W5	350.2	2624	3450	
W6	528	4200	3860	

Time-series modeling provides an output of the WEC for each wave state over 2,000sec time interval. An example of this average power output modeling is given in Fig. 7, above. We have assumed the electrical power generated directly through the 3-phase generator and rectifier occurs at 72% mechanical to electrical efficiency (manufacturer specification). Despite the addition of the flywheel, the difference between average power output

and peak output is still quite large, although the EDLC supercapacitor will be able to handle these large power spikes.

G. Desalinated Water Output

The desalination units used in combination with the WEC are (2) Schenker Zen 30's. For modeling purposes, the average water output, desalinated water and brine salinity, and power requirements are all assumed from the manufacturer's specifications. Since this is a mass-produced unit, we do not expect major deviations from these values.

We have assumed losses due to pumping and/or other parasitics (e.g., RO pump efficiencies, membrane performance) are included in the manufacturers desalinated water output specification for a given power input. Assuming a wave state characteristic from Table 1, the average desalinated water output varies widely between 0.29 and 1.0 L/m depending on the sea state. The total 5-day production is 6,210 Liters, with more than 80% produced during W3, W4, and W5 sea states. Expected total dissolved solids will be <500ppm, and a brine discharge concentration of ~70,000mg/L.

IV. MODEL VALIDATION

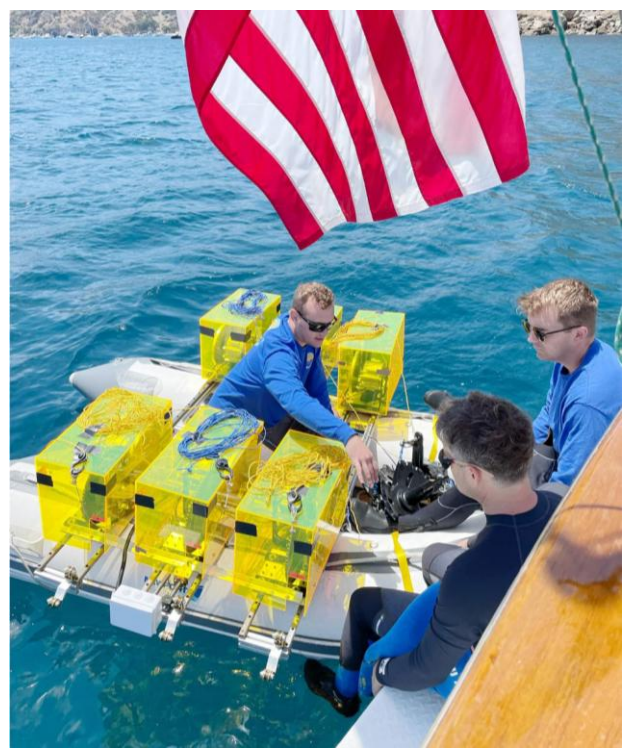


Fig. 8. A full-scale system was built and tested in the waters off Catalina Island. The deck of the mothership was used to simulate Jeannette's Pier.

A full-scale system prototype was built to demonstrate functionality of the WEC and validate the physics model presented in the section above. In this test, (6) PTO's were used to generate electricity which was then transferred to the deck of a support boat, approximately 6m above sealevel (Fig. 8).

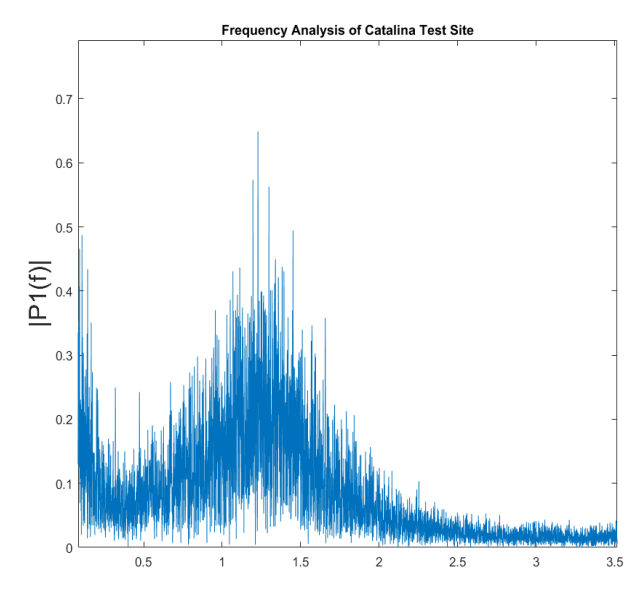


Fig. 9. IMU measured wave characteristics at Catalina test deployment area. The 'choppiness' of the waves in this region that was noted by the team is reflected in the Fast Fourier Transform output.

Significant wave heights (H_s) and frequencies (ω_m) were estimated from IMU measurements and input into the 3DOF WEC model to predict power output. The IMU was located on the WEC midplane near the measured Center of Gravity (0.75m forward of the raft transom). The wave state at the Catalina Island test site most closely resembled the W2 wave state from Table 1 with $\omega_m \sim 1.2$ rad/s and $H_s \sim 4*\sigma(H) = 0.25m$ (see Fig. 9).

The MATLAB model predicted an average power output of 84W from the PTO's and 70W delivered to the batteries. This wave state was relatively constant over an hour of testing, allowing the team to monitor 48V battery charging to estimate the average power output of the WEC. During this period, the team observed battery voltage increase from 54.1V to 54.6V. Based on the battery manufacturers charging IV curve (at 25deg and 0.5C charge rate), this corresponds to a battery capacity increase from 30% to 45% and an average power input to battery of 60W +/-20W. We expect this value to have a large uncertainty for several reasons - the ambient temperature and charge rate were not at manufacturer specification for the charging IV curve, and there is some uncertainty in the battery voltage measurement. Nevertheless, the expected and measured average power output are consistent, serving as further validation of the 3DOF WEC model and demonstration of the full-scale system operation.

The prototype testing faced limitations in data acquisition due to the complexities of the marine environment, such as the difficulty in measuring anchor line tension in real-time, obtaining precise PTO reaction torque data, and quantifying electrical losses throughout the system.

To enhance confidence in the model's accuracy, future testing will prioritize the incorporation of more detailed measurements, including direct measurement of anchor line tensions using load cells, instrumentation of the PTO system to capture reaction torque dynamics, and comprehensive monitoring of electrical parameters to assess losses and optimize power transfer efficiency.

In addition to the WEC functional demonstration, the team was able to demonstrate PTO motion under line tension in real wave conditions over the course of 48 hours. This had previously been identified as a possible technical risk during earlier design stages.

V. DISCUSSION

While the prototype demonstration was not able to access the full spectrum of wave states, the limited model validation of a single W2 wave state gives us confidence that the WEC will perform as expected in a real-world deployment. The WEC based desalination system presented here represents a simple and mobile means of producing community-scale drinking water. The production of electrical power may have utility outside of desalination in a disaster scenario. The WEC and desalination system can be deployed by two people with common equipment (SCUBA or inflatable boat), basic tools, in a variety of site conditions (beach, pier, or boat). Simple mechanical systems and available resources at the deployment site may be utilized (e.g. beach sand/rocks and other found materials) to act as anchors/mooring points for the WEC.

By utilizing COTS components wherever possible to minimize design risk and take advantage of existing supply chains for parts availability, the system may offer a lower cost alternative to existing larger marine or solar powered desalination options. Additionally, we expect that communities affected by a coastal weather event may find utility and/or re-use of the inflatable boat that forms the basis of the WEC. Estimates for the quantity of drinking water needed per person per day (L/p/d) in a post-disaster scenario varies between 1.89 and 7 L/p/d [9]. In a coastal disaster scenario, assuming a similar wave state as W1-W6, this WEC and desalination system could provide enough drinking water to sustain a community of between 200 and 400 people.

ACKNOWLEDGEMENT

The work presented here was supported by the U.S. Department of Energy's Water Power Technologies Office (WPTO) Waves to Water competition, designed to accelerate the development of small, modular, wave energy-powered desalination systems.

The authors wish to thank Amish Patel, Connor Dietz, Corey Struck, Anothony Mirabile, Rich Gangloff, Clark Beesemyer, Kyle Ross, Pete Hyde, Kevin Hyde, Tim Weed, and Mark Hammond for engineering support and assistance in WEC deployment testing.

REFERENCES

 USGCRP-II, "Impacts, Risks, and Adaptation in the United States: Fourth National Climate Assessment, Volume II," Tech.

- Rep. (U.S. Global Change Research Program, Washington, DC, 503 USA, 2018) \underline{DOI}
- Korde, Umesh A. "Enhancing the resilience of energy systems: Optimal deployment of wave energy devices following coastal storms." Journal of Renewable and Sustainable Energy 11.3 (2019). <u>DOI</u>
- Drew, Benjamin, Andrew R. Plummer, and M. Necip Sahinkaya. "A review of wave energy converter technology." (2009): 887-902. DOI
- Jenne, Scott. 2.1. 4.420-Waves to Water: A Desalination Prize. No. NREL/PR-5700-83359. National Renewable Energy Lab.(NREL), Golden, CO (United States), 2022. <u>DOI</u>
- Salmon, Rick. "Introduction to ocean waves." Scripps Institution of Oceanography, University of California, San Diego (2008). <u>DOI</u>

- 6. Finke, M., and Gerold Siedler. "Drag coefficients of oceanographic mooring components." Journal of Atmospheric and Oceanic Technology 3.2 (1986): 255-264. <u>DOI</u>
- Heddleson, C. F., D. L. Brown, and R. T. Cliffe. Summary of drag coefficients of various shaped cylinders. General Electric, Aircraft Nuclear Propulsion Department, Atomic Products Division, Technical Publications Sub-Section, 1957. <u>DOI</u>
- 8. Newman, John Nicholas. Marine hydrodynamics. The MIT press, 2018. <u>DOI</u>
- De Buck, Emmy, et al. "A systematic review of the amount of water per person per day needed to prevent morbidity and mortality in (post-) disaster settings." *PLoS One* 10.5 (2015): e0126395. DOI
- Bretschneider, C.L. 1977. On the determination of the design ocean wave spectrum. Look Lab/Hawaii 7(1), 1-23. James K.K. Look Laboratory of Oceanographic Engineering, University of Hawaii <u>DOI</u>